Glyconanosomes: Disk-Shaped Nanomaterials for the Water Solubilization and Delivery of Hydrophobic Molecules

Mohyeddin Assali,[†] Juan-José Cid,[†] Manuel Pernía-Leal,[†] Miguel Muñoz-Bravo,[‡] Inmaculada Fernández,[§] Ralf E. Wellinger,[‡] and Noureddine Khiar[†,*]

[†]Laboratory of Asymmetric Synthesis and Functional Nanosystems, Instituto de Investigaciones Químicas (IIQ), CSIC and Universidad de Sevilla, C/Américo Vepucio 49, 41092 Seville, Spain, [‡]Centro Andaluz de Biología Molecular y Medicina Regenerativa (CABIMER), 41092 Seville, Spain, and [§]Departamento de Química Orgánica y Farmacéutica, Facultad de Farmacia, Universidad de Sevilla, C/Profesor García González 2, 41012 Seville, Spain

ABSTRACT Herein, we describe the first report on a new class of disk-shaped and quite monodisperse water-soluble nanomaterials that we named glyconanosomes (GNS). GNSs were obtained by sliding out the cylindrical structures formed upon self-organization and photopolymerization of glycolipid 1 on single-walled carbon nanotube (SWCNT) sidewalls. GNSs present a sheltered hydrophobic inner cavity formed by the carbonated tails, surrounded by PEG and lactose moieties. The amphiphilic character of GNSs allows the water solubility of insoluble hydrophobic cargos such as a perylene-bisimide derivative, [60]fullerene, or the anti-carcinogenic drug camptothecin (CPT). GNS/C_{60} inclusion complexes are able to establish specific interactions between peanut agglutinin (PNA) lectin and the lactose moiety surrounding the complexes, while CPT solubilized by GNS shows higher cytotoxicity toward MCF7-type breast cancer cells than CPT alone. Thus, GNS represents an attractive extension of nanoparticle-based drug delivery systems.

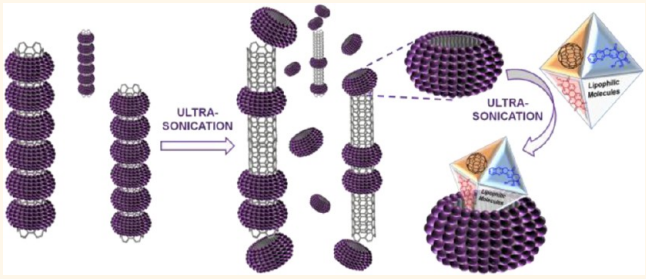

KEYWORDS: carbon nanotubes · glyconanosomes · camptothecin · drug delivery · noncovalent functionalization · [60]fullerene

During the last two decades, nanoparticle (NP)-based therapeutics have been developed for the treatment of cancer, diabetes, allergies, neurodegenerative disease, infections, and inflammations, with heavy emphasis on imaging and drug delivery.[1,2] A number of materials including polymers, dendrimers, liposomes, quantum dots, iron oxides, gold nanoparticles, and carbon nanotubes have been employed as drug carriers.[3−5] Despite the great advances achieved by this first generation of nanomaterials, the search for new tailor-made nanometric carriers with novel topologies, well-defined sizes, and improved physical and biological properties is of prime importance.[6] The general strategy used for the synthesis of NP therapeutics is based on the conjugation of conveniently functionalized payloads such as targeting agents and antitumoral drugs usually obtained through multistep chemical synthesis onto the nanoparticle surface.[7] Whereas the synthetic difficulties lie on the convenient functionalization of appropriate payloads, the design of the resulting NP therapeutics typically includes a poly(ethylene glycol) (PEG) fragment,[8] in order to reduce the rapid uptake and clearance *in vivo* by the cell mononuclear phagocytic system and an affinity ligand which permits a specific cell targeting.[9] Additionally, the overall design must contemplate the mechanism for release of the therapeutic cargo that does not denature it once the nanomedicine has reached its target tissue.[10] In some cases, the functionalization of the active principle is not possible or induces a loss of the biological activity,[11] making necessary an alternative design for the synthesis of a nanoparticle with multifunctional moieties.[6,12] Such nanoparticles contain an additional internal hydrophobic area which can host hydrophobic guest molecules such as cytotoxic

* Address correspondence to khiar@iiq.csic.es.

Received for review October 26, 2012 and accepted February 19, 2013.

Published online February 19, 2013
10.1021/nn304986x

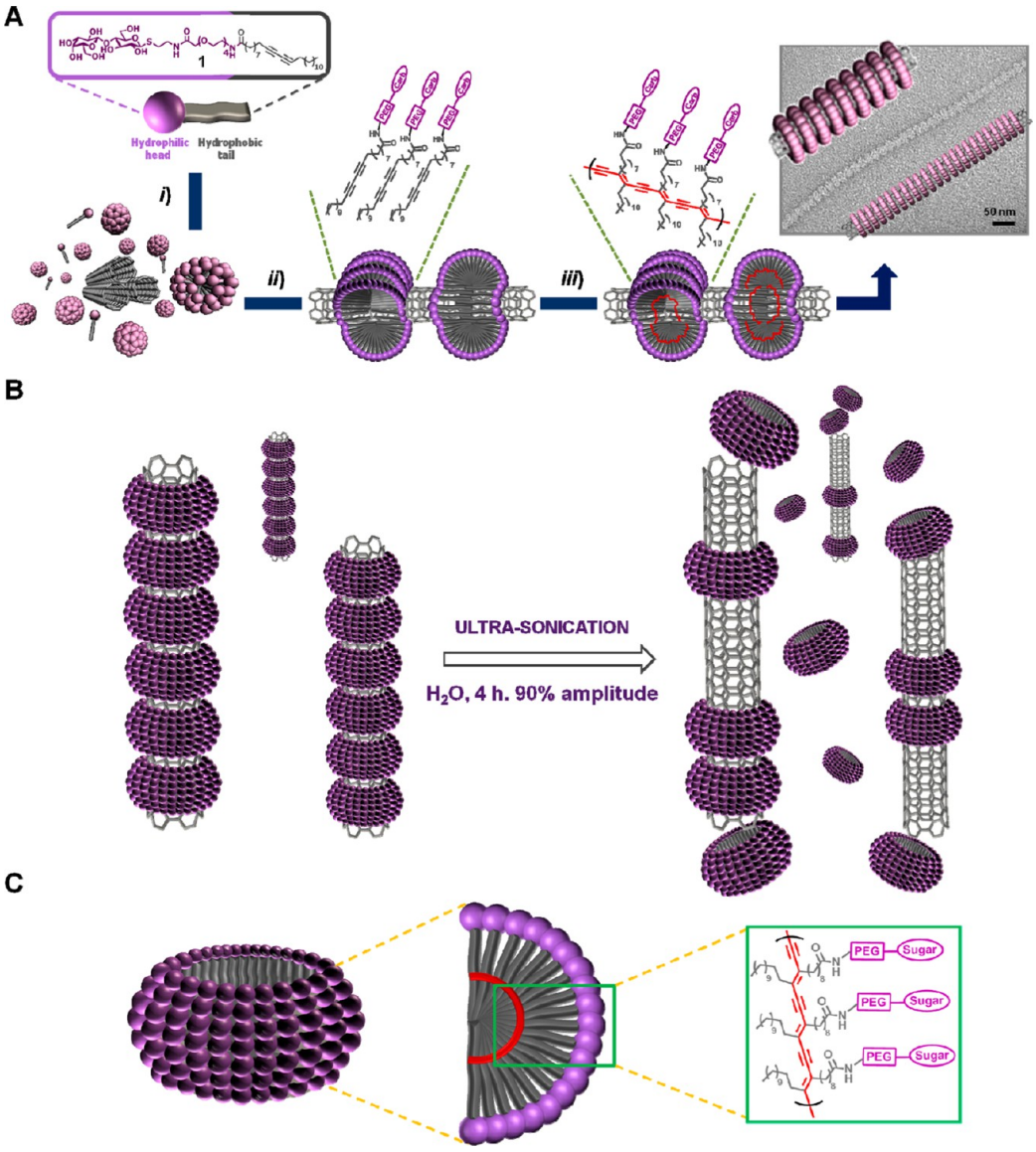

Figure 1. Procedure for SWCNT/1 nanoassembly formation and synthesis of glyconanosome (GNS). (A) (*i*) Mix of neoglycolipid 1 at its critical micelle concentration in water with SWCNTs. (*ii*) Sonication-promoted supramolecular self-assembly of neoglycolipid 1 in concentric hemimicelles around SWCNTs. (*iii*) Intermolecular photopolymerization of neoglycolipid 1 hemimicelles into homogeneous glyconanorings (GNRs). Above, the TEM micrograph of SWCNT/1 nanoassemblies and their idealized representative figures. (B) Schematic representation of the ultrasonication setup for obtaining GNS. (C) Structural and chemical composition of a glyconanosome (GNS).

or image-enhancing agents, metal nanoparticles, or other therapeutics.[10,13] Such nanodevices can operate as general nanovectors for poorly soluble drugs or drug candidates currently accounting for 40−70% of new chemical entities discovered by high-throughput screening,[14] with no need of additional chemical functionalization as no release mechanism of the active principle is required.

On the basis of these premises, in the present work, we report the design and synthesis of new disk-shaped water-soluble and monodisperse nanomaterials we coined glyconanosomes (GNS), consisting of two fundamental functional areas, central for their application as smart nanovectors for drug delivery. GNSs can be produced by a simple method through the supramolecular self-organization and photopolymerization of diacetylenic-based glycolipid on the SWCNT surface, thus working the latter as molecular scaffolds that moreover dictate their shape and topology. Subsequent subtraction of SWCNTs leads to functional GNSs, which enable the solubilization of poorly soluble molecules in water, permit selective interaction with specific receptors, and have the potential to improve the bioactivity of anticancer drugs.

RESULTS AND DISCUSSION

Due to the excellent properties of biocompatible CNTs to shuttle a wide range of biologically active molecules insides the cells,[15,16] we have recently reported a bottom-up approach for the water solubilization and

biofunctionalization of CNTs (Figure 1),[17] based on the self-organization of amphiphilic molecules on the CNT sidewall.[18−21] Beside the lactose headgroup, the designed neoglycolipid **1** contains a 25 carbon-based hydrophobic tail for efficient van der Waals interactions with the CNT, a tetraethyleneglycol spacer that enhances the hydrophilicity of the molecule,[22] and with a diacetylenic function known to photopolymerize under very smooth conditions (see Figure 1A).[23] By a simple sonication using a common ultrasound bath, neoglycolipid **1** was capable of facilitating deaggregation of SWCNTs, giving rise to stable dispersions of assembled SWCNT/**1** nanoconstructs consisting mainly of individual or small bundles of sugar-coated nanotubes, as evidenced by TEM (Figure 1A), AFM (see Supporting Information Figure S2), and UV−vis−NIR (see Supporting Information Figure S1) analyses. Interestingly, TEM analyses showed that compound **1** self-assembled on the SWCNT surface in a supramolecular fashion, resulting in rings made of rolled-up half cylinders (Figure 1A, step *ii*). The photopolymerization of the diacetylene function upon ultraviolet irradiation (254 nm) afforded a conjugated polydiacetylene backbone of alternating enyne groups (Figure 1A, step *iii*), which rigidified the inner core of each hemimicelle, resulting in robust glyconanorings (GNRs) polymerized around the nanotube in an abacus-like geometry. These new assemblies or multicomposites that form even more stable water solutions than those of nonpolymerized precursors have been recently studied by atomic force microscopy (AFM), which revealed that polymerized SWCNT/**1** nanoconstructs consist mainly of individual and small bundles of nanotubes whose surfaces are completely covered by striations of hemimicelles with diameters of 45−50 nm (see the Supporting Information for recorded AFM micrographs).

The high stability of the obtained supramolecular assemblies in different solvents, buffers, and in water solutions (80 °C for one week) clearly indicates that SWCNTs coated with polymerized polydiacetylene-based glyconanorings behave as a single entity and not as a dynamic supramolecular association between the glycolipid and the nanotube. On the basis of these observations, we postulated that the polymerized glyconanorings could be pulled off from the tube (Figure 1B), affording fairly monodisperse disk-shaped nanomaterials with a hydrophobic inner core surrounded by a hydrophilic tetraethyleneglycol chain capped by a biodetectable lactose moiety (Figure 1C).

Ultrasounds have been used for the deaggregation, dispersion, and weakening of the interactions of apolar chemical entities in polar solvents,[24] as well as for cutting and homogenizing CNT sizes.[25] We thus applied ultrasounds with a high-power sonication tip for glyconanoring extraction (500 W power) during 4 h at 5 s on/off intervals (Figure 1B). Following this optimized

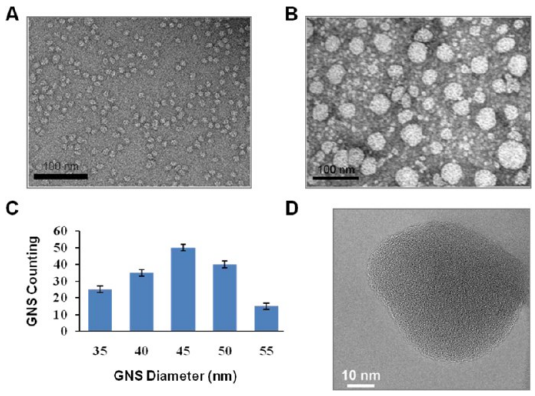

Figure 2. Microscopic characterization of GNSs. (A) TEM micrograph of neoglycolipid 1 micelles. (B) TEM micrograph of GNSs. (C) Size distribution of GNSs. (D) HR-TEM micrograph of a GNS.

procedure, a black precipitate and a homogeneous dark gray dispersion were obtained. Glyconanorings were recovered by ultracentrifugation (17 968*g*), precipitating the whole carbonaceous material while the extracted water-soluble glyconanorings remained in the colorless aqueous supernatant. Analysis of the carbonaceous precipitate reveals the formation of larger disk-shaped carbon-based rings with an average diameter of 200−250 nm in length formed by the self-folding and superposition of CNTs during the extraction of the glyconanorings and whose nature and characterization will be discussed in more detail elsewhere.

TEM analyses of the supernatant show a collection of circular nanostructures with a diameter matching that of rings on the functionalized SWCNTs (diameter 35−55 nm; see Figure 2B and histogram in Figure 2C). On the other hand, TEM analysis of a water solution of neoglycolipid **1** above its CMC revealed the formation of circular structures with 12 nm diameter (Figure 2A), ruling out the possibility that the extracted nanostructures are micelles formed by the amphiphilic neoglycolipid monomer **1**.

After evaporation and lyophilization, the glyconanorings were obtained free from carbonaceous materials in 48% yield based on the starting neoglycolipid **1** used (see Supporting Information for supplementary details). ^{1}H NMR analysis (see Supporting Information) of the obtained glyconanorings reveals a single spin system reminiscent of that of the starting glycolipid in agreement with the symmetry of the biomaterial. Further high sonication under the same conditions as those used for the synthesis of the glyconanorings did not disrupt their structure as monitored by NMR (see Supporting Information). Additional stability test experiments checked by ^{1}H NMR analysis show that the glyconanorings remain stable under a wide range of temperatures (20−60 °C), pH (2.2−11.7), and buffer conditions, highlighting their potential biological applications. Thus, the small polydispersity observed

(Figure 2B) probably arises from the variability in the supramolecular self-organization of glycolipid **1** on the nanotube surface (Figure 1, step *ii*), which can enclose an individual SWCNT or small bundles of nanotubes with different size.

These spherical objects are named glyconanosomes (GNS), as they possess singular structural properties (Figures 1C and 2D) appropriate for targeted drug delivery.[10,12] Indeed, the external surface of the obtained GNSs comprises tetraethlyeneglycol chains that make them highly soluble in water. GNSs are covered by an array of sugars, which in addition to enhancing their water solubility endow them with the ability to establish selective and effective interactions with lectins for selective cell adhesion.[26,27] Most importantly, GNSs feature a central hydrophobic area that allows them to bind and accommodate a wide range of hydrophobic molecules (Figure 3). Similarly to other cavitand-type architectures such as cyclodextrins, calixarenes, and cucurbiturils, GNSs exhibit a high potential as drug carriers through dynamic host–guest association–dissociation equilibrium.

Solubility Experiments with Perylene-Bisimide and C_{60}. To demonstrate that GNSs have the potential to solubilize hydrophobic agents, we first evaluated its capacity to dissolve the commercially available perylene-bisimide derivative *N,N′*-dipentyl-3,4,9,10-perylenedicarboximide **2** (Figure 4A). This compound exhibits interesting optoelectronic properties and has been therefore widely applied within materials science,[28] as well as for pharmacological and biomedical purposes.[29] Water solubility, an essential property for these applications, was partially solved by either inserting polar side chains on the perylene bay positions[30] or introducing different substituents on the imide positions.[31] Nevertheless, as both approaches result in a loss of their physical properties,[32] we reasoned that GNSs might provide an alternative method to make these kinds of compounds water-soluble without modifying their optoelectronic properties.

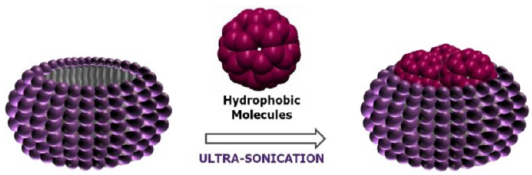

Figure 3. Schematic representation of the ultrasonication-induced inclusion of hydrophobic C_{60}, a perylene-bisimide derivative, or camptothecin inside the GNS cavity.

We generated GNS/**2** inclusion complexes by ultrasonication of 4.0 mg of **2** in 1.0 mg/mL solution of GNSs in Milli-Q water (1.0 mL) for 10 min, followed by ultracentrifugation at 17 968*g*. Excess of **2** precipitated as a dark red solid (Figure 4B), allowing the decantation of a GNS/**2**-enriched homogeneous red-orange supernatant (Figure 4C). To demonstrate the presence of the perylene-bisimide molecule inside the lipophilic GNS cavity, UV–vis spectrum of the supernatant was analyzed (Figure 4D). The supernatant showed the typical absorption pattern of deaggregated perylene-bisimide derivatives solved in organic solvents at high dilution, suggesting a stable GNS/**2** interaction allowing for the water solubilization of 3,4,9,10-perylenedicarboximide **2** in its active form.

Next, we assessed the aqueous solubilization of C_{60}, a promising compound expected to be useful in a plethora of applications in materials science and pharmaceuticals.[33,34] However, strong intermolecular van der Waals interactions and poor solubility in common organic solvents, especially in water,[35] limit its bioapplications. As it is the case for the perylene-bisimide derivative, several strategies have been developed to water solubilize C_{60}, including covalent and noncovalent functionalizations[36,37] that unfortunately lead in most cases to a partial loss of its physical properties.[36]

A GNS/C_{60} inclusion complex was obtained by a similar procedure to that used for the perylene-bisimide dye, affording a yellow aqueous supernatant (Figure 5A). The GNS/C_{60} inclusion complex was further characterized by UV–vis absorption where an initial excess of C_{60} was titrated against an increasing amount of GNSs (Figure 5B). As expected, the more GNS was added, the more C_{60} could be solubilized, resulting

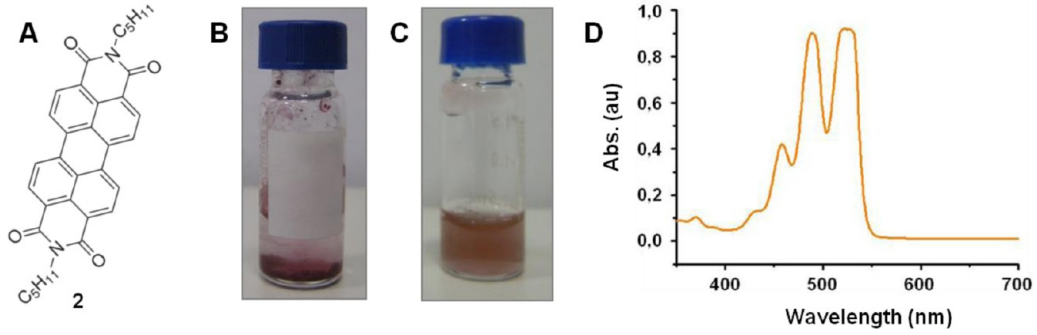

Figure 4. Synthesis and characterization of GNS/perylene-bisimide inclusion complex. (A) Structure of perylene-bisimide 2. (B) Photograph of vial with perylene derivative 2 in water. (C) Photograph of vial with the yellow-orange aqueous supernatant containing the GNS/2 inclusion complex. (D) UV–vis absorption spectrum of the GNS/2 inclusion complex.

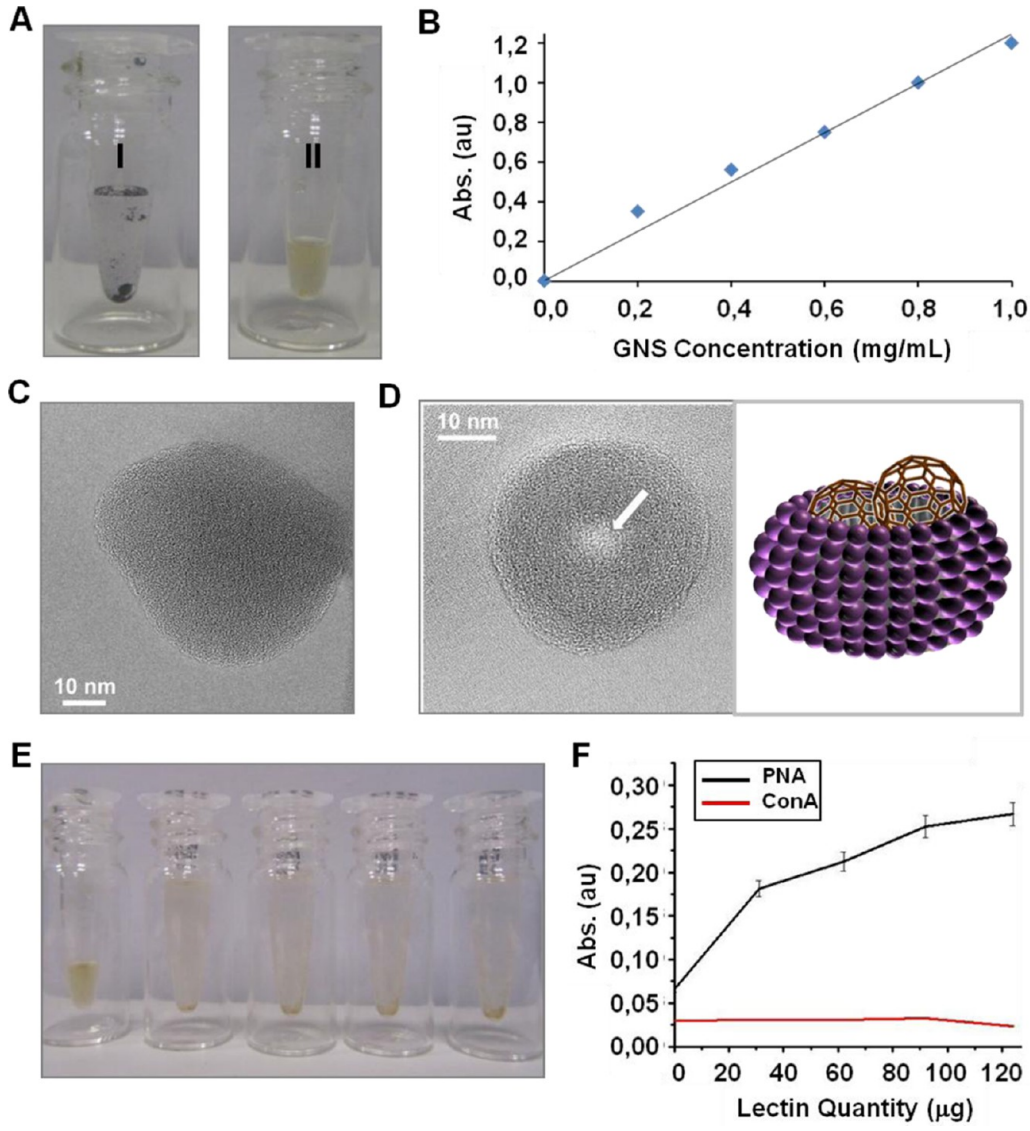

Figure 5. Preparation, characterization, and selective interaction with PNA lectin of GNS/C_{60} inclusion complex. (A) C_{60} in water (I) and aqueous solution of GNS/C_{60} (II). (B) Plot of absorbance recorded at 342 nm of GNS/C_{60} aqueous supernatants *versus* concentration values of starting GNS (in mg/mL). (C) TEM micrograph of a GNS. (D) TEM micrograph of a C_{60}/GNS complex and its figurative representation. (E) Image of GNS/C_{60}/PNA aggregates for turbidity assays. (F) Turbidity assays of incubated GNS/C_{60}/PNA (black curve) and GNS/C_{60}/ConA (red line) aggregates *versus* lectin added (in μg) by registering the absorbance values at 450 nm.

in a linear increase in C_{60} in the supernatant. The supernatant was further characterized comparing GNS and the GNS/C_{60} complex by high-resolution transmission electronic microscopy (HR-TEM; compare Figure 5C,D). Interestingly, we observed an area exhibiting a low electronic density in the middle of the GNS/C_{60}, shown as a "hole" on the HR-TEM image (arrow). This hole is consistent with the low electronic density of the packed C_{60} spheres, thus suggesting the proficient incorporation of C_{60} into GNSs.

Selective Interaction of GNS/C_{60} Complex with Peanut Agglutinin Lectin. The selective recognition of sugars by lectins allowed us to test the ability of glyconanosome to establish the interaction with specific receptors.[26,27] The peanut agglutinin lectin (PNA) from *Arachis hypogaea* was shown to specifically interact with lactose epitopes. Therefore, we performed a GNS/C_{60}/PNA interaction study by turbidity assays (Figure 5E). As a control, we used Concanavalin A (ConA), a lectin known to selectively recognize α-mannopyranoside, α-glucopyranoside, and to a lesser extent α-*N*-acetylglucosamine, but not β-lactose.[38,39] Mixing GNS/C_{60} with ConA neither caused the formation of a precipitate nor increased absorption at 450 nm (Figure 5F). However, the turbidity increased with increased PNA concentrations, suggesting a specific and dose-dependent interaction between the lectin and the GNS lactose moieties. The multiple interactions of PNA with GNS/C_{60} led to the agglutination and precipitation of the complex GNS/C_{60}/PNA leaving a colorless supernatant (Figure 5E).

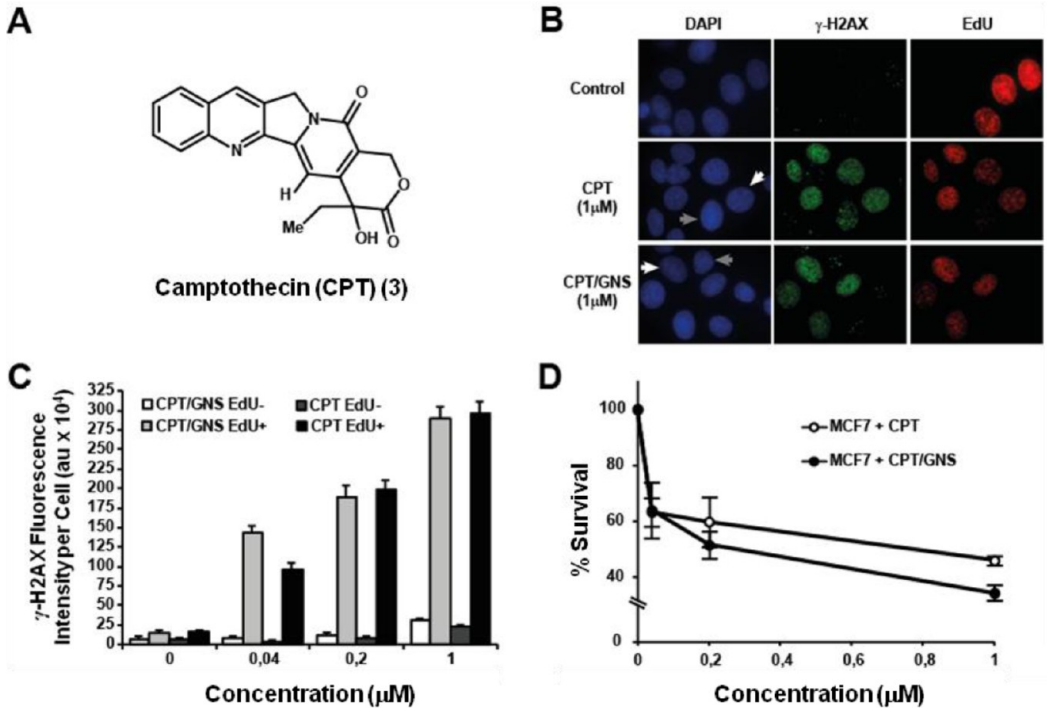

Figure 6. DNA-damage response and cell survival upon CPT or GNS/CPT treatments on MCF7 cell cultures. (A) Chemical structure of camptothecin (3). (B,C) DNA-damage response after 2.5 h with CPT or GNS/CPT treatment. Representative images showing cells co-staining for nuclear DNA (DAPI, blue), phosphorylated γ-H2AX (green), and 5-ethynyl-2′-deoxyuridine (EdU, red). Quantification of the γ-H2AX fluorescence intensity per nucleus in proliferating (EdU+, white arrows) and in nonproliferating (EdU−, gray arrows) cells. The mean ± SEM of three independent experiments is represented. (D) Graphic showing the average of MCF7 cell survival upon 2.5 h treatment with CPT or GNS/CPT. The data represent the mean ± SEM of three independent experiments.

Solubility and Stabilization Experiments with Camptothecin (CPT). Finally, we applied GNSs to solubilize the quinoline alkaloid camptothecin (CPT) **3** in water (Figure 6A). CPT is a natural cytotoxic compound with high anticarcinogenic activity against breast, colon, ovary, and lung tumors.[40] Unfortunately, this compound suffers many therapeutic limitations including poor stability, solubility, and preponderance of a less active carboxylate form at physiologic pH.[41] The synthesis of CPT analogues with improved water solubility, such as irinotecan, exhibits a significant loss of the antitumoral activity,[42] making the development of alternative methods necessary for the solubilization and stabilization of native CPT.

In a similar fashion to that accomplished for the perylene-bisimide derivative and [60]fullerene, 0.2 mg of CPT was sonicated in an aqueous GNS solution (5.0 mL) for 1 h. Then, the resulting mixture was ultracentrifuged (17 968*g*), precipitating the excess CPT and remaining fluorescent supernatant that contained CPT in the form of inclusion complex GNS/CPT. To determine the concentration of CPT incorporated into the GNSs, we measured the absorbance at the absorption maximum of CPT (369 nm)[43] in the supernatant and determined a CPT concentration of 55.2 μM (see Supporting Information for further details), a value higher than those obtained with most hydrophobic hosts developed so far.[44] Taking into account the starting amount of GNS set up, this value corresponds to a 48% efficacy of GNS to catch and host CPT in the hydrophobic internal cavity.

To assess the capacity of the GNS/CPT inclusion complex to release the CPT payload after dilution, a solution of the complex was dialyzed against a biological RPMI-1640 medium. By plotting the absorbance values at 369 nm outside the membrane at different times, a sigmoid curve was tailored (see Supporting Information Figure S5) from which a maximum value of CPT release of about 38.6% was attained after 120 min, highlighting the suitability of GNSs as stabilizer nanocontainers for the CPT release and delivery in biomedical assays against cancer-associated pathologies.

GNS/CPT Complex as a Medical Nanovehicle with Improved Toxicity to MCF7 Breast Cancer Cells. In order to compare the cellular DNA-damage response to CPT *versus* GNS/CPT treatment, we monitored DNA-damage-dependent phosphorylation of histone H2AX (γ-H2AX, Figure 6B,C). MCF7 human breast cancer-derived cell cultures were treated for 2.5 h with each antitumoral agent, that is, CPT or GNS/CPT at concentrations ranging from 0.04 to 1 μM of active CPT, in the presence of the modified nucleoside 5-ethynyl-2′-deoxyuridine (EdU) for concomitant labeling of proliferating cells. Nuclear DNA staining revealed that the CPT as well as GNS/CPT-mediated γ-H2AX response was mainly restricted to proliferating cells (Figure 6B). It is important to note

that this response was dose-dependent in such a way that the level of γ-H2AX increased to a similar extent when raising the CPT or GNS/CPT concentrations from 0.04 to 1 μM (see quantification, Figure 6C). Thus, the GNS/CPT complex neither impeded the uptake nor lowered the biological activity of CPT.

Next we assessed a cell viability study of CPT *versus* GNS/CPT-treated MCF7 cells by colony formation assay (Figure 6D). Cell cultures were treated with either different DMSO solutions of CPT or water solutions of GNS/CPT at identical concentrations ranging from 0.04 to 1 μM for 2.5 h. Importantly, the higher the GNS/CPT concentrations used, the higher the achieved toxicity as compared to CPT alone. Then, and more importantly, when using just a 1 μM solution for every agent, the GNS/CPT complex killed more than 65% of the MCF7 cells (34% survival), while less than 55% of MCF7 cells were affected by CPT alone (46% survival). These results suggest that the GNS/CPT interaction improves the anti-carcinogenic activity of CPT. It is worthy to mention that the GNS/CPT samples could be stored up to 3 months at room temperature without a notable loss of biological activity, although this observation does not explain why GNS/CPT presents a higher antitumoral activity. On the basis its molecular target (a blocking effect on the active center of type-I topoisomerase, enzyme involved in the controlled cutting of the DNA strand during the replication process),[45] CPT toxicity is imperatively restricted to proliferating cells. Depending both on cell density and growth conditions, in agreement with our data that about 30–40% of the total cell number corresponds to proliferating cells.[46] It is worthy to remark that the doubling time of tumorgenic cell cultures exceeds by far the 2.5 h treatment period, and upon extracellular CPT withdraw, the cells would have enough time to activate the detoxification activities, thus providing a rapid drop in the intracellular CPT levels.[47] An attractive possibility would be that the GNS/CPT interaction could interfere with cellular CPT detoxification mechanisms in such a way that the intracellular CPT retention time gets increased, prolonging the span and release time of the drug.

CONCLUSION

In summary, we have prepared novel and biologically active nanomaterials by ultrasonication-assisted sliding of neutral glyconanorings out of their assemblies with SWCNTs. The new disk-shaped nanomaterials, called glyconanosomes (GNSs), with a 35–55 nm diameter have a hydrophobic inner core surrounded by a hydrophilic tetraethyleneglycol chain capped by a biodetectable lactose moiety and are thus well-suited for drug delivery. We show that GNSs are able to solubilize and stabilize a wide range of lipophilic structures like C_{60}, perylene-bisimide, or camptothecin. The GNS/C_{60} inclusion complexes are able to establish a positive and specific interaction with the peanut agglutinin (PNA) lectin, highlighting the suitability of GNS as a nanovector for active drug delivery. The GNS/CPT inclusion complex provides increased CPT stability and water solubility at physiological pH, resulting in an improved killing of MCF7 breast cancer cells. The demonstration that CPT retained its *in vitro* anticancer activity when complexed to GNS established that drugs contained inside the hydrophobic GNS core may be slowly released in their active form. As the method uses SWCNTs as template to shape the internal cavity and the supramolecular self-organization and photopolymerization of diacetylenic-based glycolipid to modulate the topology and function of the rings, it is straightforward to imagine the synthesis of a broad range of GNSs with tailored sizes and activities using CNTs with varied diameters and neoglycolipids functionalized with other active principle. On the other hand, recent investigations have confirmed the prime importance of carbohydrates in important biological events including cell–cell communication, cell adhesion, fertilization, differentiation, development, inflammation, tumor cell metastasis, and pathogen infections.[38,39] Thus, the GNSs which are covered by a dense carbohydrate array can be used as synthetic multivalent systems to treat pathologies mediated by carbohydrate–lectin interactions.[48] The highly convergent and modular approach developed for the synthesis of compound **1** allows a rapid preparation of a large number of neoglycoconjugates by using different 2-aminoethyl thioglycosides. In this sense, we have recently reported a one-step synthesis of 2-aminoethyl thioglycosides,[17] which will permit us to fine-tune the GNSs' outer face for an optimal and specific interaction with biologically relevant receptors. These studies are under investigation in our laboratories.

METHODS AND EXPERIMENTS

Synthesis of Glyconanosomes. In a typical experiment, glycolipid **1** (1.0 mg) was dissolved in Milli-Q water (1.0 mL) above its critical micellar concentration. Then, SWCNTs (1.0 mg) purchased from Carbon Solutions Company were added, and the mixture was sonicated in an ultrasound bath for 1 h. The resulting dark black precipitate (consisting of amorphous carbon and catalysts) was removed by low-speed centrifugation (825*g*, for 5 min) and decantation. The afforded stable black aqueous supernatant, composed by functionalized SWCNT/glycolipid **1**, was subject to irradiation under a UV lamp at 254 nm for 24 h, thus promoting the photopolymerization of the diyne functionalities into the ring-shaped polymeric poly(diacetylene) derivatives around the SWCNT sidewalls. Subsequently, a second high-speed centrifugation of the solution (17 968*g*, for 10 min) was accomplished, settling for this case a black precipitate consisting of supramolecularly functionalized SWCNT/glycolipid **1** nanoassemblies while glycolipid in excess remained in the supernatant. The centrifugation/decantation

process was repeated four times, giving rise to pure SWCNT/**1** nanoconstructs. Afterward, so as to slide the glyconanorings (GNRs) out of the tubes, the supramolecular SWCNT/**1** assemblies were suspended in Milli-Q water and ultrasonicated with a high-power sonication tip (500 W), during 4 h at 5 s on/off intervals. An ulterior centrifugation at high speed (17 968*g*, for 10 min) enabled decantation to separate the precipitated carbonaceous material from the water-soluble glyconanosomes (GNSs) contained in the supernatant.

Cytotoxicity Assay. MCF7 cells were grown in RPMI-1640 medium supplemented with 10% FBS and standard antibiotics. Upon 2.5 h CPT or GNS/CPT treatment, cell survival assays were performed as described previously.[49] Prior to inmunofluorescence microscopy, MCF7 cells were treated during 2.5 h with 10 μM of EdU and varying CPT or GNS/CPT, respectively. Cells were fixed with 4% *p*-formaldehyde (w/v) in PBS for 10 min. Coverslips were washed with PBS and immunostained with primary antibodies against γ-H2AX (Millipore). Appropriate Alexa Fluor 488 (green) conjugated secondary antibodies (1:1000) were purchased from Invitrogen. After rinsing the coverslips with 1% BSA in PBS (w/v), cells were inmunostained with an Alexa Fluor 647 (red) azide through a "click" reaction for EdU detection.[50] Nuclear DNA was stained with DAPI (blue) for 1 min.

Conflict of Interest: The authors declare no competing financial interest.

Acknowledgment. This work was supported by the Ministerio de Economía y Competitividad (Grant Nos. CTQ2010-21755-CO2-01 and BFU2010-21339), the Junta de Andalucía (Grant Nos. P07-FQM-2774 and P08-CTS-04297). We acknowledge CITIUS for TEM, AFM, and NMR facilities, and Dr. Rosaria Brescia from Instituto Italiano di Tecnologia in Geneva for HR-TEM measurements. M.A. thanks the MAEC-AECID for a PhD scholarship. J.-J.C. thanks CSIC for the postdoctoral JAE DOC scholarship, and M.M.-B. thanks the Junta de Andalucía for predoctoral training grant. We thank Hélène Gaillard and Daniel Fitzgerald for critical reading of the manuscript.

Supporting Information Available: Experimental procedures for the synthesis of compound **1**, GNS, the inclusion complexes, turbidity assay, CPT release, NMR spectra of **1** and GNSs, stability experiments, and additional AFM and TEM images. This material is available free of charge *via* the Internet at http://pubs.acs.org.

REFERENCES AND NOTES

1. Irvine, D. J. Drug Delivery: One Nanoparticle, One Kill. *Nat. Mater.* **2011**, *10*, 342–343.
2. Doane, T. L.; Burda, C. The Unique Role of Nanoparticles in Nanomedicines: Imaging, Drug Delivery and Therapy. *Chem. Soc. Rev.* **2012**, *41*, 2885–2911.
3. O'Malley, W.; Kubeil, M.; Graham, B.; Stephan, H.; Spiccia, L. Nanomaterials: Applications in Cancer Imaging Therapy. *Adv. Mater.* **2011**, *23*, H18–H40.
4. De Jong, W. H.; Borm, P. J. A. Drug Delivery and Nanoparticles: Applications and Hazards. *Int. J. Nanomed.* **2008**, *3*, 133–149.
5. Theranostic Nanomedicine Special Issue. *Acc. Chem. Res.* **2011**, *44*, 841−1134.
6. Godin, B.; Tasciotti, E.; Liu, X. W.; Serda, R. E.; Ferrari, M. Multistage Nanovectors: From Concept to Novel Imaging Contrast Agents and Therapeutics. *Acc. Chem. Res.* **2011**, *44*, 979–989.
7. Mout, R.; Moyano, D. F.; Rana, S.; Rotello, V. Surface Functionalization of Nanoparticles for Nanomedicine. *Chem. Soc. Rev.* **2012**, *41*, 2539–2544.
8. Moros, S.; Hernáez, B.; Garet, E.; Dias, J. T.; Sáez, B.; Grazú, V.; González-Fernández, A.; Alonso, C.; De la Fuente, J. M. Monosaccharides *versus* PEG-Functionalized NPs: Influence in the Cellular Uptake. *ACS Nano* **2012**, *6*, 1565–1577.
9. Debbage, P. Targeted Drugs and Nanomedicine: Present and Future. *Curr. Pharm. Des.* **2009**, *15*, 153–172.
10. Ding, M.; Li, J.; He, X.; Song, N.; Tan, H.; Zhang, Y.; Zhou, L.; Gu, Q.; Deng, H.; Fu, Q. Molecular Engineered Super-Nanodevices: Smart and Safe Delivery of Potent Drugs into Tumors. *Adv. Mater.* **2012**, *24*, 3639–3645.
11. Jain, R. K. Transport of Molecules, Particles and Cells in Solid Tumors. *Annu. Rev. Biomed. Eng.* **1999**, *1*, 241–263.
12. Godin, B.; Driessen, W. H.; Proneth, B.; Lee, S. Y.; Srinivasan, S.; Rumbaut, R.; Arap, W.; Pasqualini, R.; Ferrari, M.; Decuzzi, P. An Integrated Approach for the Rational Design of Nanovectors for Biomedical Imaging and Therapy. *Adv. Genet.* **2010**, *69*, 31–64.
13. Nyström, A. M.; Wooley, K. L. The Importance of Chemistry in Creating Well-Defined Nanoscopic Embedded Therapeutics: Devices Capable of the Dual Functions of Imaging and Therapy. *Acc. Chem. Res.* **2011**, *44*, 969–978.
14. Porter, C. J. H.; Trevaskis, N. L.; Charman, W. N. Lipids and Lipid-Based Formulations: Optimizing the Oral Delivery of Lipophilic Drugs. *Nat. Rev. Drug Discovery* **2007**, *6*, 231–248.
15. Liu, Z.; Tabakman, S. M.; Chen, Z.; Dai, H. Preparation of Carbon Nanotube Conjugates for Biomedical Applications. *Nat. Protoc.* **2009**, *4*, 1372–1382.
16. Hong, S. Y.; Tobias, G.; Al-Jamal, K. T.; Ballesteros, B.; Ali-Boucetta, H.; Lozano-Pérez, S.; Nellist, P. D.; Sim, R. B.; Finucane, C.; Mather, S. J.; *et al.* Filled and Glycosylated Carbon Nanotubes for *In Vivo* Radioemitter Localization and Imaging. *Nat. Mater.* **2010**, *9*, 485–490.
17. Khiar, N.; Pernía-Leal, M.; Baati, R.; Ruhlmann, C.; Mioskowski, C.; Schultz, P.; Fernández, I. Tailoring Carbon Nanotube Surfaces with Glyconanorings: New Bionanomaterials with Specific Lectin Affinity. *Chem. Commun.* **2009**, 4121–4123.
18. Richard, C.; Balavoine, F.; Schultz, P.; Ebbesen, T. W.; Mioskowski, C. Supramolecular Self-Assembly of Lipid Derivatives on Carbon Nanotubes. *Science* **2003**, *300*, 775–778.
19. Islam, M. F.; Rojas, E.; Bergey, D. M.; Johnson, A. T.; Yodh, A. G. High Weight Fraction Surfactant Solubilization of Single-Wall Carbon Nanotubes in Water. *Nano Lett.* **2003**, *3*, 269–273.
20. Ke, P. U. Fiddling the String of Carbon Nanotubes with Amphipiles. *Phys. Chem. Chem. Phys.* **2007**, *9*, 439–447.
21. Thauvin, C.; Rickling, S.; Schultz, P.; Célia, H.; Meunier, S.; Mioskowski, C. Carbon Nanotubes as Templates for Polymerized Lipid Assemblies. *Nat. Nanotechnol.* **2008**, *3*, 743–748.
22. Corti, M.; Cantù, L.; Brocca, P.; Del Favero, E. Self-Assembly in Glycolipids. *Curr. Opin. Colloid Interface Sci.* **2007**, *12*, 148–154.
23. Ahn, D. J.; Kim, J.-M. Fluorogenic Polydiacetylene Supramolecules: Immobilization, Micropatterning, and Application to Label-Free Chemosensors. *Acc. Chem. Res.* **2008**, *41*, 805–816.
24. Yu, J.; Grossiord, N.; Koning, C. E.; Loos, J. Controlling the Dispersion of Multi-Wall Carbon Nanotubes in Aqueous Surfactant Solution. *Carbon* **2007**, *45*, 618–623.
25. Zheng, M.; Jagota, A.; Semke, E. D.; Diner, B. A.; Mclean, R. S.; Lustig, S. R.; Richardson, R. E.; Tassi, N. G. DNA-Assisted Dispersion and Separation of Carbon Nanotubes. *Nat. Mater.* **2003**, *2*, 338–342.
26. Banerjee, R.; Das, K.; Ravishankar, R.; Suguna, K.; Surolia, A.; Vijayan, M. Conformation, Protein−Carbohydrate Interactions and a Novel Subunit Association in the Refined Structure of Peanut Lectin−Lactose Complex. *J. Mol. Biol.* **1996**, *259*, 281–296.
27. André, S.; Frisch, B.; Kaltner, H.; Desouza, D. L.; Schuber, F.; Gabius, H. J. Lectin-Mediated Drug Targeting: Selection of Valency, Sugar-Type (Gal/Lac), and Spacer Length for Cluster Glycosides as Parameters To Distinguish Ligand Binding to C-Type Asialoglycoprotein Receptors and Galectins. *Pharm. Res.* **2000**, *17*, 985–990.
28. Huang, C.; Barlow, S.; Marder, S. R. Perylene-3,4,9,10-tetracarboxylic Acid Diimides: Synthesis, Physical Properties, and Use in Organic Electronics. *J. Org. Chem.* **2011**, *76*, 2386–2407.
29. Yin, M.; Kuhlmann, C. R.; Sorokina, K.; Li, C.; Mihov, G.; Pietrowski, E.; Koynov, K.; Klapper, M.; Luhmann, H. J.; Müllen, K.; *et al.* Novel Fluorescent Core−Shell Nanocontainers for Cell Membrane Transport. *Biomacromolecules* **2008**, *9*, 1381–1389.
30. Qu, J.; Kohl, C.; Pottek, M.; Müllen, K. Ionic Perylenetetracarboxdiimides: Highly Fluorescent and Water-Soluble

Dyes for Biolabeling. *Angew. Chem., Int. Ed.* **2004**, *43*, 1528–1531.
31. Hahn, U.; Engmann, S.; Oelsner, C.; Ehli, C.; Guldi, D. M.; Torres, T. Immobilizing Water-Soluble Dendritic Electron Donors and Electron Acceptors—Phtalocyanines and Perylenediimides—onto Single Wall Carbon Nanotubes. *J. Am. Chem. Soc.* **2010**, *132*, 6392–6401.
32. Zhang, X.; Rehm, S.; Safont-Sempere, M.; Würthner, F. Vesicular Perylene Dye Nanocapsules as Supramolecular Fluorescent pH Sensor Systems. *Nat. Chem.* **2009**, *1*, 623–629.
33. Innocenzi, P.; Brusatin, G. Fullerene-Based Organic–Inorganic Nanocomposites and Their Applications. *Chem. Mater.* **2001**, *13*, 3126–3139.
34. Partha, R.; Conyers, J. L. Biomedical Applications of Functionalized Fullerene-Based Nanomaterials. *Int. J. Nanomed.* **2009**, *4*, 261–275.
35. Ruoff, R. S.; Tse, D. S.; Malhotra, R.; Lorents, D. C. Solubility of C_{60} in a Variety of Solvents. *J. Phys. Chem.* **1993**, *97*, 3379–3383.
36. Diederich, F.; Thilgen, C. Covalent Fullerene Chemistry. *Science* **1996**, *271*, 317–323.
37. Babu, S. S.; Möhwald, H.; Nakanishi, T. Recent Progress in Morphology Control of Supramolecular Fullerene Assemblies and Its Applications. *Chem. Soc. Rev.* **2010**, *39*, 4021–4035.
38. Lis, H.; Sharon, N. Lectins: Carbohydrate-Specific Proteins That Mediate Cellular Recognition. *Chem. Rev.* **1998**, *98*, 637–674.
39. Simanek, E. E.; McGarvey, G. J.; Jablonski, J. A.; Wong, C. H. Selectin-Carbohydrate Interactions: From Natural Ligands to Designed Mimics. *Chem. Rev.* **1998**, *98*, 833–862.
40. Oberlies, N. H.; Kroll, D. J. Camptothecin and Taxol: Historic Achievements in Natural Products Research. *J. Nat. Prod.* **2004**, *67*, 129–135.
41. Fassberg, J.; Stella, V. J. A Kinetic and Mechanistic Study of the Hydrolysis of Camptothecin and Some Analogues. *J. Pharm. Sci.* **1992**, *81*, 676–684.
42. Rivory, L. P.; Robert, J. Molecular, Cellular, and Clinical Aspects of the Pharmacology of 20(*S*)Camptothecin and Its Derivatives. *Pharmacol. Ther.* **1995**, *68*, 269–296.
43. Sanna, N.; Chillemi, G.; Gontrani, L.; Grandi, A.; Mancini, G.; Castelli, S.; Zagotto, G.; Zazza, C.; Barone, V.; Desideri, A. UV–Vis Spectra of the Anticancer Camptothecin Family Drugs in Aqueous Solution: Specific Spectroscopic Signatures Unraveled by a Combined Computational and Experimental Study. *J. Phys. Chem. B* **2009**, *113*, 5369–5375.
44. Ma, D.; Hettiarachchi, G.; Nguyen, D.; Zhang, B.; Wittenberg, J. B.; Zavalij, P. Y.; Briken, Y.; Isaacs, L. Acyclic Cucurbit[*n*]uril Molecular Containers Enhance the Solubility and Bioactivity of Poorly Soluble Pharmaceuticals. *Nat. Chem.* **2012**, *4*, 503–510.
45. Redinbo, M. R.; Stewart, L.; Kuhn, P.; Champoux, J. J.; Hoi, W. G. J. Crystal Structures of Human Topoisomerase I in Covalent and Non-covalent Complexes with DNA. *Science* **1998**, *279*, 1504–1513.
46. Hartog, H.; Van Der Graaf, W. T. A.; Boezen, H. M.; Wesseling, J. Treatment of Breast Cancer Cells by IGF1R Tyrosine Kinase Inhibitor Combined with Conventional Systemic Drugs. *Anticancer Res.* **2012**, *32*, 1309–1318.
47. Rasheed, Z. A.; Rubin, E. H. Mechanisms of Resistance to Topoisomerase I-Targeting Drugs. *Oncogene* **2003**, *22*, 7296–7304.
48. Witczak, Z. J., Nieforth, K. A. *Carbohydrates in Drug Design*; Marcel Dekker Inc.: New York, 1997.
49. Sartori, A. A.; Lukas, C.; Coates, J.; Mistrik, M.; Fu, S.; Bartek, J.; Baer, R.; Lukas, J.; Jackson, S. P. Human CtIP Promotes DNA End Resection. *Nature* **2007**, *450*, 509–514.
50. Salic, A.; Mitchison, T. J. A. Chemical Method for Fast and Sensitive Detection of DNA Synthesis *in Vivo*. *Proc. Natl. Acad Sci. U.S.A.* **2008**, *105*, 2415–2420.